Physica B ∎ (∎∎∎∎) ∎∎∎–∎∎∎

Contents lists available at ScienceDirect

Physica B

journal homepage: www.elsevier.com/locate/physb

Damage formation in Ge during Ar^+ and He^+ implantation at 15 K

M. Hayes [a,*], A. Schroeter [b], E. Wendler [b], W. Wesch [b], F.D. Auret [a], J.M. Nel [a]

[a] Department of Physics, University of Pretoria, Pretoria, South Africa
[b] Institut für Festkörperphysik, Friedrich-Schiller-Universität, Jena, Germany

ARTICLE INFO

PACS:
00.00.Xx
11.11.Yy
61.72.Cc
61.72.Ti
61.82.Fk
81.05.Cy
85.30.−z

Keywords:
Implantation
Defects
Ions
RBS
Channelling
Ge

ABSTRACT

Ar^+ and He^+ ions were implanted into Ge samples with (1 0 0), (1 1 0), (1 1 1) and (1 1 2) orientations at 15 K with fluences ranging from 1×10^{11} to $1\times10^{14}\,cm^{-2}$ for the Ar^+ ions and fluences ranging from 1×10^{12} to $6\times10^{15}\,cm^{-2}$ for the He^+ ions. The Rutherford backscattering (RBS) technique in the channelling orientation was used to study the damage built-up in situ. Implantation and RBS measurements were performed without changing the target temperature. The samples were mounted on a four axis goniometer cooled by a close cycle He cryostat. The implantations were performed with the surface being tilt 7° off the ion beam direction to prevent channelling effects. After each 300 keV Ar^+ and 40 keV He^+ implantation, RBS analysis was performed with 1.4 MeV He^+ ions.

For both the implantation ions, there is about no difference between the values found for the damage efficiency per ion for the four different orientations. This together with the high value (around 5 times higher than that found in Si), gives rise to the assumption of amorphous pocket formation per incident ion, i.e. direct impact amorphization, already at low implantation fluences. At higher fluences, when collision cascades overlap, there is a growth of the already amorphized regions.

© 2009 Published by Elsevier B.V.

1. Introduction

Germanium has been the preferred host for most of the early studies on defects in semiconductors. The research was driven by the search for sensitive detectors for gamma radiation [1]. Defects and defect formation in Ge, being in the shade over the last two decades, have recently generated new interest because of their potential applications. The low effective mass of holes in Ge has opened up the possibility of using Ge in ultrafast complimentary metal-oxide-semiconductor devices [2]. This, in turn, has sparked renewed interest in the properties of defects in Ge because defects ultimately determine the performance of devices. Germanium-on-insulator (GeOI), which combines high mobility of charge carriers with the advantage of a silicon-on-insulator (SOI) structure, is an attractive integration platform for the future integrated circuit technology. Also, due to its low lattice mismatch with GaAs, III–V compound transistors as well as optoelectronic functions can be integrated on GeOI [3].

Because of the poor identification of defects in Ge, the interpretation of electrical and optical data, especially those obtained at low-temperature radiation experiments, has been given by a common analogy with the known defects in Si. However, there are many striking dissimilarities between defect production and annealing processes in both materials [4]. In order to study purely ion-induced effects during implantation of materials, thermal influences have to be suppressed by reducing the target temperature and by preventing sample heating between implantation and measurement. The laboratory at the Friedrich-Schiller-Universität in Jena has a special target chamber which fulfils these conditions [5]. The aim of this investigation is thus to gain understanding in the primary mechanisms of damage formation during Ar^+ and He^+ ion irradiation of different orientations of Ge.

2. Experimental

The Ge samples used during this investigation were purchased form UMICORE [(1 0 0), (1 1 0) and (1 1 1) orientations] and CrysTec [(1 1 2) orientation]. They were all n-type, those from UMICORE doped with Sb to a level of $8\times10^{14}\,cm^{-3}$ for the (1 0 0) orientation, $8\times10^{13}\,cm^{-3}$ for the (1 1 0) orientation, $6\times10^{14}\,cm^{-3}$ for the (1 1 1) orientation while those from CrysTec were nominally undoped. The Ge samples were mounted on a four axis goniometer and the implantations were performed with the surface tilted 7° off the ion beam direction to prevent channelling. During the implantation of the 300 keV Ar^+ ions to fluences ranging from 1×10^{11} to $1\times10^{14}\,cm^{-2}$, and the 40 keV He^+ ions to

* Corresponding author. Tel.: +27 12 641 2503; fax: +27 12 305 43045288.
E-mail address: michael.hayes@pbmr.co.za (M. Hayes).

0921-4526/$ - see front matter © 2009 Published by Elsevier B.V.
doi:10.1016/j.physb.2009.09.021

ARTICLE IN PRESS

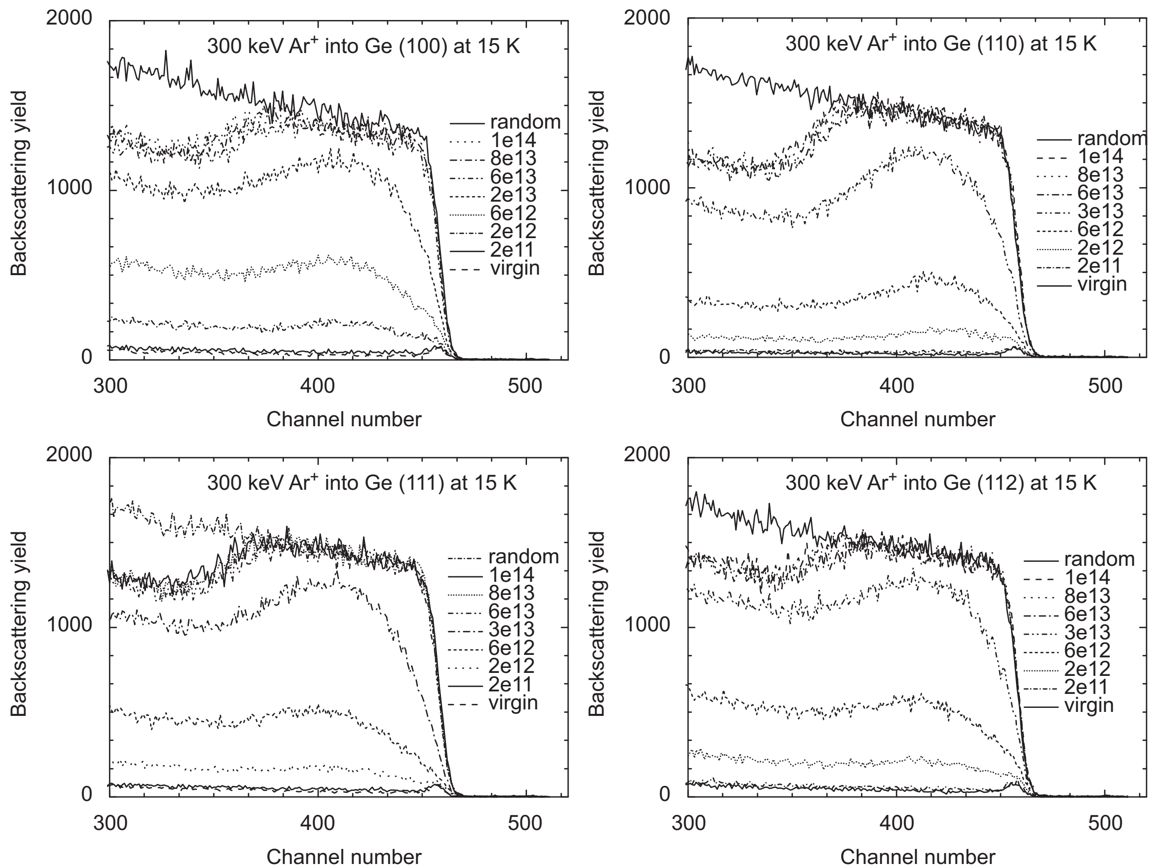

Fig. 1. Energy spectra of 1.4 MeV He^+ ions backscattered from four different orientations of Ge implanted with Ar^+ implanted Ge [(1 0 0)—top left, (1 1 0)—top right, (1 1 1)—bottom left and (1 1 2)—bottom right].

fluences ranging from 1×10^{12} to $6\times10^{15}\,cm^{-2}$, the implantation rate was kept below $2\times10^{10}\,cm^{-2}\,s^{-1}$. Using 1.4 MeV He^+ ions, the Rutherford backscattering (RBS) technique in the channelling orientation with a backscattering angle of 170° was used to study the damage build-up in situ. Both implantation and RBS measurements were performed with the samples cooled by a close cycle He cryostat to 15 K and without changing the target temperature between implantation and analysis. After each implantation, RBS analysis was performed before the next implantation.

Applying the computer code DICADA (based on the discontinuous model of dechannelling [6,7]), the relative concentration of displaced lattice atoms, n_{da} (for short called relative defect concentration) versus depth z was calculated from the RBS spectra assuming the displaced atoms to be randomly distributed within the lattice cell.

3. Results

Fig. 1 shows the energy spectra of the 1.4 MeV He^+ ions backscattered from the four orientations of Ge samples, implanted with Ar^+ ions to various fluences N_I at 15 K. Although there are slight variations in the shape of the backscattered spectra from the four different orientations, it can be seen that the yield increases continuously with increasing ion fluence and reaches the random level at $N_I\approx6\times10^{13}\,cm^{-2}$, indicating the formation of a buried amorphous layer. Both implantations and measurements were performed at 15 K. For clarity, the spectra measured for some ion fluences are omitted. The same tendency was observed for spectra from Ge samples implanted with He^+ ions, where the yield reaches the random level at $N_I\approx3\times10^{15}\,cm^{-2}$.

From the channelling spectra the relative defect concentration of displaced lattice atoms, n_{da}, versus depth was calculated using the DICADA code [6,7] and are plotted in Fig. 2. For these calculations a random distribution of the displaced lattice atoms is assumed which is reasonable for low temperature implants [5]. A Debye temperature of 374 K was used. The depth profile of the energy density primarily deposited in nuclear processes as calculated using the TRIM code [8] is also included in arbitrary units for comparison. As can be seen, good agreement was found between the calculated and measured damage distributions with respect to the position of the maximum and the broadness of the distribution for both the Ar^+ and He^+ ion implantations.

For the analysis of the fluence dependence of defect production the defect concentration in the maximum of the distribution was taken. In order to improve statistics, n_{da}, was averaged over a depth of 0.08 μm in the depth regions between 0.11 and 0.19 μm for the four different orientations of Ge implanted with Ar^+ ions and between 0.16 and 0.24 μm for the four different orientations of Ge implanted with He^+ ions. The resulting values n_{da}^{max} versus the ion fluence N_I are depicted in Fig. 3. It is clear from Fig. 3 that the defect concentration n_{da}^{max} increase linearly with increasing fluence N_I until amorphization is reached. As expected, it was found that the higher mass Ar^+ ions have a higher damage efficiency than He^+ ions.

A summary of the resulting cross-sections for direct impact damage production, P, versus the melting temperature of Ar^+ ion implantations at 15 K into some III–V compounds found in the literature [5,9–14] as well as for Ge and Si [14] are given in Fig. 4. These materials can be divided into two groups, i.e. those where

Please cite this article as: M. Hayes, et al., Physica B (2009), doi:10.1016/j.physb.2009.09.021

ARTICLE IN PRESS

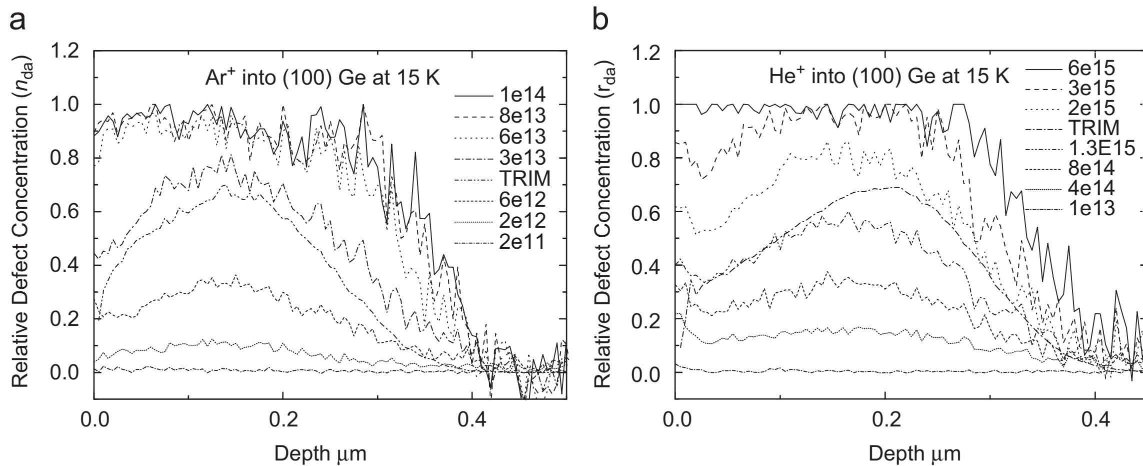

Fig. 2. Relative concentration of displaced lattice atoms, n_{da}, versus depth for (a) 300 keV Ar^+ ions and (b) 40 keV He^+ ions implanted into (1 0 0) Ge at 15 K. The energy density deposited in nuclear processes as calculated using the TRIM code is also included.

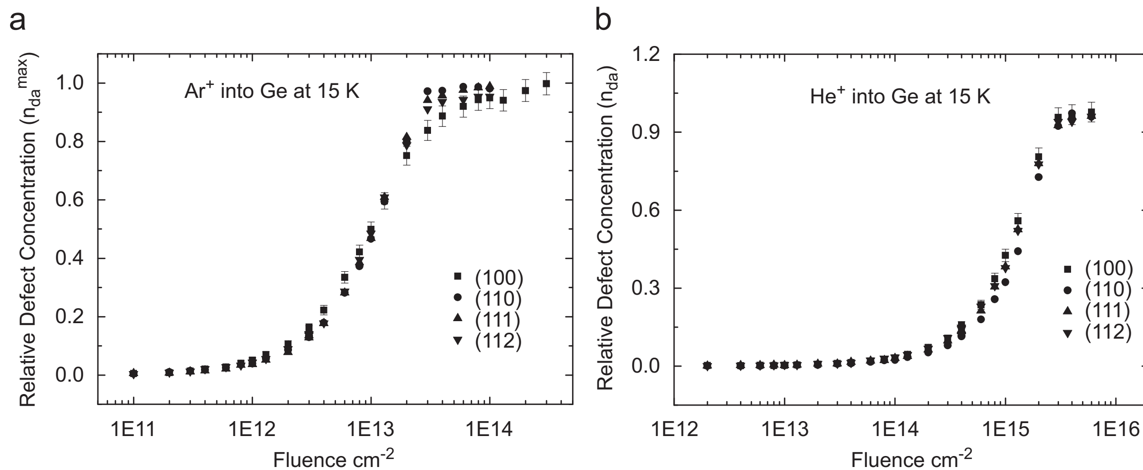

Fig. 3. Relative concentrations of displaced lattice atoms, n_{da}^{max}, in the maximum of the distribution versus the (a) Ar^+ ion fluence and (b) He^+ ion fluence, N_I.

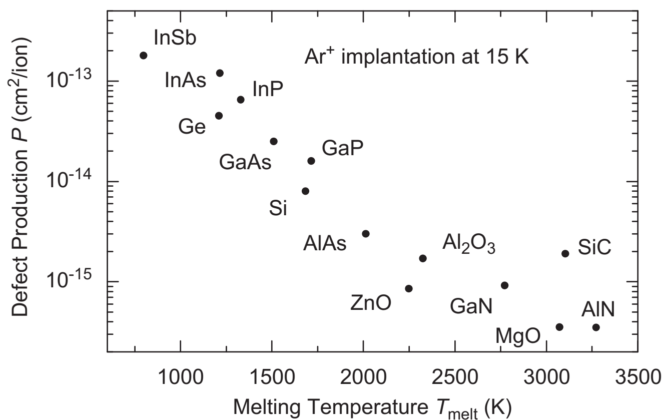

Fig. 4. Summary of cross-sections for damage production P versus the melting temperature of the materials for Ar^+ implantations at 15 K into various III–V compounds as well as Ge and Si.

the defect concentration increases smoothly to a maximum value and those where the defect concentration remains low and increase only slightly with increasing fluence [10]. From Fig. 4, it is clear that Ge also belongs to the first group with weaker bond strengths where stimulated growth dominates when the collision cascades start to overlap, forcing the amorphization of the implanted layer.

4. Conclusions

There is no significant difference in the damage efficiency per ion found for the four different orientations of either the Ar^+ or He^+ ion implanted Ge. This, together with the high value (5 times higher than that found in Si), gives rise to the assumption of amorphous pocket formation per incident ion, i.e. direct impact amorphization, already at low implantation fluences. At higher fluences, when collision cascades overlap, there is a growth of the already amorphized regions.

References

[1] J. Weber, M. Hiller, E.V. Lavrov, Mater. Sci. Semiconductor Processing 9 (2006) 564.
[2] R. Hull, J.C. Bean (Eds.), Germanium Silicon: Physics and Materials, Semiconductors and Semimetals, vol. 56, Academic Press, San Diego, 1999.

Please cite this article as: M. Hayes, et al., Physica B (2009), doi:10.1016/j.physb.2009.09.021

ARTICLE IN PRESS

[3] T. Akatsu, C. Deguet, L. Sanchez, F. Allibert, D. Rouchon, T. Signamarcheix, C. Richtarch, A. Boussagol, V. Loup, F. Mazen, J.-M. Hartmann, Y. Vampidelli, L. Clavelier, F. Letertre, N. Kernevez, C. Mazure, Mater. Sci. Semiconductor Processing 9 (2006) 444.
[4] V. Emtsev, Mater. Sci. Semiconductor Processing 9 (2006) 580.
[5] B. Breeger, E. Wendler, W. Trippensee, Ch. Schubert, W. Wesch, Nucl. Instr. Meth. B 174 (2001) 199.
[6] K. Gärtner, Nucl. Instr. Meth. B 132 (2001) 147.
[7] K. Gärtner, Nucl. Instr. Meth. B 227 (2005) 522.
[8] J.F. Ziegler, J.P. Biersack, U. Littmark, The Stopping and Range of Ions in Solids, Pergamon, New York, 1985.
[9] E. Wendler, A. Kamarou, E. Alves, K. Gärtner, W. Wesch, Nucl. Instr. Meth. B 206 (2003) 1028.
[10] E. Wendler, W. Wesch, Nucl. Instr. Meth. B 242 (2006) 562.
[11] E. Wendler, K. Gärtner, W. Wesch, Nucl. Instr. Meth. B 257 (2007) 488.
[12] C.S. Schnohr, E. Wendler, K. Gärtner, K. Ellmer, W. Wesch, Nucl. Instr. Meth. B 2506 (2006) 85.
[13] E. Wendler, B. Breeger, W. Wesch, Nucl. Instr. Meth. B 175–177 (2001) 83.
[14] E. Wendler, A. Schroeter, 2007, private communication.

Please cite this article as: M. Hayes, et al., Physica B (2009), doi:10.1016/j.physb.2009.09.021